CENTER FOR CONNECTED AND AUTOMATED TRANSPORTATION

Report No. ICT-20-011 November 2018

Project Start Date: November 2016

Project End Date: September 2018

CDF Analysis and Prediction Model for Air Resistance on Platooned Freight Trucks

by
Ruifeng She
Yanfeng Ouyang
Imad L. Al-Qadi
University of Illinois at Urbana–Champaign

DISCLAIMER

Funding for this research was provided by the Center for Connected and Automated Transportation under Grant No. 69A3551747105 of the U.S. Department of Transportation, Office of the Assistant Secretary for Research and Technology (OST-R), University Transportation Centers Program. The contents of this report reflect the views of the authors, who are responsible for the facts and the accuracy of the information presented herein. This document is disseminated under the sponsorship of the Department of Transportation, University Transportation Centers Program, in the interest of information exchange. The U.S. Government assumes no liability for the contents or use thereof.

Suggested APA Format Citation:

She, R., Ouyang, Y., & Al-Qadi I. L. (2018). *CDF analysis and prediction model for air resistance on platooned freight trucks* (Report No. ICT-20-011). Illinois Center for Transportation. https://doi.org/10.36501/0197-9191/20-011

Contacts:

Ruifeng She
University of Illinois at Urbana–Champaign
B235 Newmark Civil Engineering Laboratory
205 North Mathews Avenue, Urbana, IL 61801
rshe2@illinois.edu
(217) 300-1488
https://ict.illinois.edu

CCAT
University of Michigan Transportation Research Institute
2901 Baxter Road
Ann Arbor, MI 48152
uumtri-ccat@umich.edu
(734) 763-2498
www.ccat.umtri.umich.edu

TECHNICAL REPORT DOCUMENTATION PAGE

1. Report No. ICT-20-011	**2. Government Accession No.** N/A	**3. Recipient's Catalog No.** N/A
4. Title and Subtitle CDF Analysis and Prediction Model for Air Resistance on Platooned Freight Trucks		**5. Report Date** November 2018 **6. Performing Organization Code** N/A
7. Authors Ruifeng She, Yanfeng Ouyang, and Imad L. Al-Qadi		**8. Performing Organization Report No.** ICT-20-011 UILU-ENG-2020-2011
9. Performing Organization Name and Address Illinois Center for Transportation Department of Civil and Environmental Engineering University of Illinois at Urbana-Champaign 205 North Mathews Avenue, MC-250 Urbana, IL 61801		**10. Work Unit No.** N/A **11. Contract or Grant No.** Grant No. 69A3551747105
12. Sponsoring Agency Name and Address Center for Connected and Automated Transportation University of Michigan Transportation Research Institute 2901 Baxter Road Ann Arbor, MI 48152		**13. Type of Report and Period Covered** N/A **14. Sponsoring Agency Code** Center for Connected and Automated Transportation

15. Supplementary Notes

Funding under Grant No. 69A3551747105 U.S. Department of Transportation, Office of the Assistant Secretary for Research and Technology (OST-R), University Transportation Centers Program
https://doi.org/10.36501/0197-9191/20-011

16. Abstract

Motivated by autonomous and connected vehicle technology, truck platooning has significant economic benefits on the freight transportation industry. Lower average fuel consumption can be achieved due to the reduced air-drag force experienced by the platoon during operation. This report presents the procedure and results of computational fluid dynamics (CFD) analysis and aims to evaluate the stationary air drag on platooned freight trucks. CFD simulation is performed on paired truck models using the Ansys Fluent software to quantify the effect of positioning on drag force. A prediction model is proposed to evaluate the average air drag on platoons of various sizes and spatial configurations. The results of this study showed the loss of air-drag reduction in platooning when trucks are separated and misaligned and suggested the platoon size needed to achieve maximum drag reduction.

17. Key Words Connected and Autonomous Vehicles, Truck Platooning, Computational Fluid Dynamics, Aerodynamic	**18. Distribution Statement** No restrictions. This document is available through the National Technical Information Service, Springfield, VA 22161.

19. Security Classif. (of this report) Unclassified	**20. Security Classif. (of this page)** Unclassified	**21. No. of Pages** 17 + appendix	**22. Price** N/A

Form DOT F 1700.7 (8-72) **Reproduction of completed page authorized**

ACKNOWLEDGMENT, DISCLAIMER, MANUFACTURERS' NAMES

This project was conducted in cooperation with the Center for Connected and Automated Transportation and the Illinois Center for Transportation. The contents of this report reflect the view of the authors, who are responsible for the facts and the accuracy of the data presented herein. The contents do not necessarily reflect the official views or policies of CCAT or ICT. This report does not constitute a standard, specification, or regulation. Trademark or manufacturers' names appear in this report only because they are considered essential to the object of this document and do not constitute an endorsement of the product by CCAT or ICT.

TABLE OF CONTENTS

LIST OF FIGURES

LIST OF TABLES

CHAPTER 1: INTRODUCTION

OVERVIEW

Road transportation with trucks is the dominant mode for freight transportation in the United States, thanks to a mature highway network. Heavy duty vehicles (HDVs), such as class-8 tractor trailers or above, are mostly used for shipments with a gross weight above 30,000 lbs. In 2014, 360 billion vehicle miles of freight shipments have been made by heavy duty trucks (HDTs) within the United States (U.S. DOT, 2010). At the same time, HDVs are the most energy-consuming surface transportation mode due to their low fuel economy. In 2014, HDVs had an average fuel economy of 6.4 miles/gal. Consequently, 29.1 billion gallons were consumed by HDVs, and 7 million metric tons of greenhouse gases were emitted (U.S. DOT, 2010).

Fuel consumption of HDVs consists of aerodynamic loss (35–55%), rolling resistance (30–40%), powertrain loss, grade changes, and accessory loss (e.g., lighting and air-conditioning systems). Among those, the main contributor of engine power consumption is aerodynamic loss (drag), which scales with operational speed at a higher pace (power of 3) than with rolling resistance (power of 2). The industry has made great efforts to reduce transportation costs by introducing aerodynamic designs on HDVs such as skirts, retractable trailers, and boat tails.

Recently, attention has been drawn to improve freight transportation from a systematic perspective by implementing technology in connected and autonomous vehicles (CAVs). With intervehicle communication and control devices, the motion of individual trucks can be precisely controlled. This allows for smaller intervehicle separation in CAV truck platoons than human-driven ones. Generally, human drivers have a reaction time of 2.5 sec, which translates into traffic regulations requiring a separation of 500 ft or higher for safety concerns. Platooned traffic brings superior advantages, including higher freight throughput and better safety and stability due to minimized dependency on human factors and actions.

Another major benefit from truck platooning is the reduction of fuel consumption due to air drag. According to the National Renewable Energy Laboratory, 76.6% of vehicle miles are suitable for platooning lasting longer than 15 min and traveling at a relatively constant speed. For trucks, 6.4% of total energy and 1.5 billion gallons of fuel can be saved (Lammert et al., 2014). HDVs are mostly used for shipments below 250 mi, because other modes such as railroads become more favorable for longer distances. However, these short trips usually concentrate on a small number of corridors between certain trade hubs. This further enhances the practicability of truck platooning.

The objective of this report is to quantify the influence of platooning patterns on the air resistance suffered by a series of HDTs. First, the air resistance of automated HDTs at different platooning configurations will be evaluated using a computational fluid dynamics (CFD) simulation. The methodology, procedure, and results will be exhibited. Second, a mathematical model is developed to predict the gross air drag of a platoon with a given size and configuration.

LITERATURE REVIEW

Extensive effort has been seen on analyzing the effect of platooning on drag reduction for various types of vehicles. Because of a lack of analytical approaches, the most acknowledged method to evaluate aerodynamic characteristics of vehicles is to conduct a wind-tunnel test with a realizable setup. Zabat et al. (1995) conducted a wind-tunnel test on passenger vans with platoon sizes of two, three, and four vehicles. The results exhibited a nonlinear behavior of drag ratio with respect to an isolated truck at different separations. The trailing vehicle(s) in a platoon receives damped marginal air-drag reduction, revealing the asymptotic benefits achieved on gross (average) fuel consumption by platooning with more than two trucks. The marginal gain from adding the fourth truck, which is the largest platoon size tested, has proven to be very small compared to two trucks. Consequently, the asymptote is expected to be achieved by a platoon of five or six vehicles.

Research groups have conducted tests for HDVs from the perspective of fuel consumption. Bonnet and Fritz (2007) conducted tests on a pair of tractor trailers and showed the negative influence of separation distances on fuel efficiency. The trailing truck receives a drag reduction of 27% compared to the leading truck. The leading truck is located 24 ft ahead and traveled at 50 mph, which is a typical scenario for CAV-equipped trucks. Yoshida et al. (2010) conducted similar experiments in Japan for truck platoons under a path-following control and observed a similar pattern.

Findings on the aerodynamic characteristics of platoons with lateral offset are much more limited, on the other hand. To the best of the authors' knowledge, the only to-scale test addressing the influence of lateral offset was conducted by Marcu and Browand in 1998. A misaligned platoon with three vehicles was tested with the middle truck shifted aside by a small amount. The result exhibits a much more complicated, yet also asymptotic influence, on air-drag reduction.

Recent tests were conducted by the National Renewable Energy Laboratory on fuel economy of HDVs. Standard evaluation approaches on fuel efficiency provided a numerical connection between air drag and fuel consumption. Additionally, the researchers developed simplified models that enabled numerical simulations with acceptable accuracy. Ahmed et al. (1984) introduced the Ahmed body, a rectangular blunt body that closely resembles car models in terms of aerodynamic characteristics as verified in wind-tunnel tests. This simplified geometry has been commonly accepted by computational researchers because of its simplicity and high fidelity.

The existent test results and studies encourage the idea of platooning in freight transportation. However, scarce effort has been made to predict the gain from large-sized platoons because of high testing cost and inability to obtain analytical solutions. This report exhibits an attempt to provide a prediction model for large-size platoons based on CFD simulations of paired trucks. The test results in the literature served as benchmarks to validate CFD simulations.

CHAPTER 2: SIMULATIONS AND RESULTS

ANSYS FLUENT OVERVIEW

A series of CFD simulations were conducted to evaluate the drag reduction on a pair of trucks with different configurations (separation and lateral offset). The models were created and combined in Ansys Workbench 17 and solved by Ansys Fluent, a CFD solver dedicated to fluid flow problems.

The simulated body (Ahmed body) was created in the SpaceClaim 3D Modeler (SCM), which was integrated in the Ansys CFD package. This modeler is available in Ansys Workbench 16 and later versions, and it is capable of modeling complex geometries in an interactive graphical user interface (GUI). In addition, the original parametric modeler, DesignModeler (DM), in the earlier versions is also available and serves a similar purpose. The prototype was designed in SCM, and an enclosed Boolean operation was performed in DM. The latter step creates the computational domain from the test body.

The geometry created (either by integrated modeler or external ones such as AutoCAD) is passed down to Ansys Meshing. Refinements are required if the mesh does not pass quality checks. Refinements include adjusting face sizes, adaptive repairing, and adding local refinement boxes. Refinement boxes are generally used behind each truck body, where the mesh is regenerated with smaller elements and the wake region is anticipated.

The accepted mesh will then be passed to the CFD solver, Ansys Fluent. Ansys Fluent is a robust CFD solver that handles various fluid flow models, including cavitation, heat transfer, and fluid-structure interaction. It is especially strong at solving turbulence problems with numerous pre-imbedded models. This project aims to study turbulence formulation behind the truck body. The turbulence is incompressible and without phase change, and heat transfer is negligible and not of interest. Therefore, the turbulence model is well defined by currently available model(s) and can be processed by the Fluent solver with acceptable computational cost and fidelity.

SIMULATION PROCEDURE

MODELING

The geometry of the prototype used in this project is a rectangular body with a blunted head, as shown in Figure 1. The body had a scale of 1:20 to the truck model. In addition, the prototype was created per the drawing in FHWA (2004), as shown in Figure 2. Miscellaneous external features were simplified or omitted, such as wheels, hangers, and mirrors. The curved design of the driving chamber is captured by the blunted head of radius 0.01 m and 0.04 m.

The test body is duplicated and arranged according to the configuration to be tested. Figure 3 shows the case of 20 ft separations and 4 ft lateral offset. The computational domain is a rectangular enclosure, which, according to Lanfrit (2005), should extend three truck lengths away from the body

in the front, five in the rear, three on the sides, and one on the top. A separation of 1/4 truck height is set below the body to replace the height of the wheels.

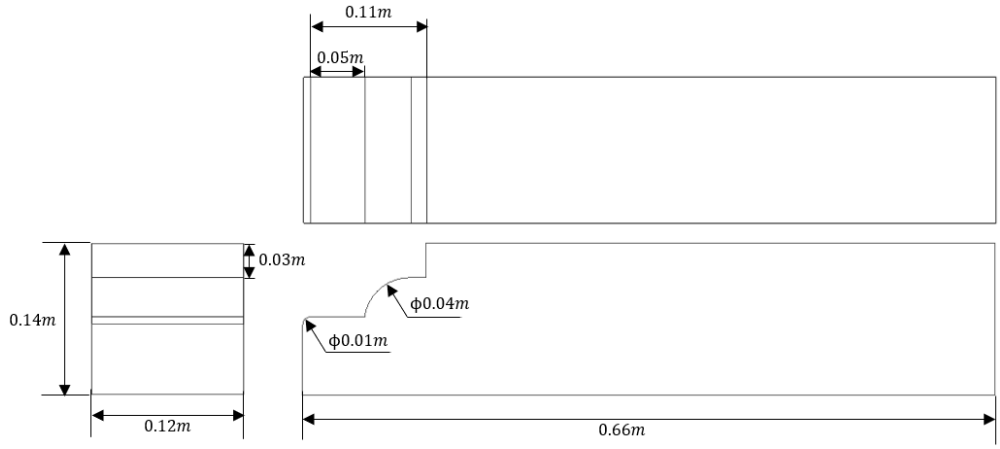

Figure 1. Photo. Multiview and dimensions of test body.

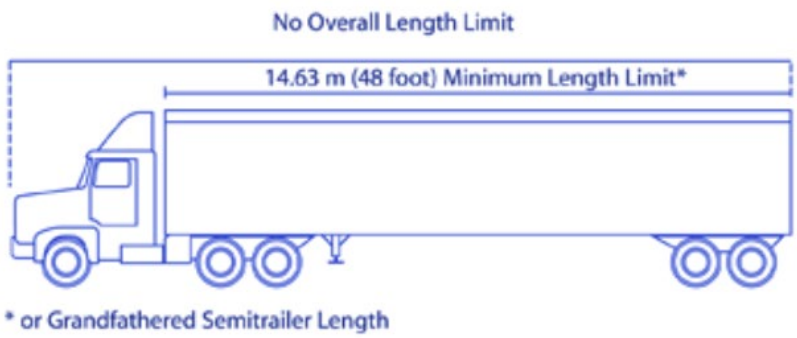

Figure 2. Photo. Class 8 dimension by FHWA regulation.

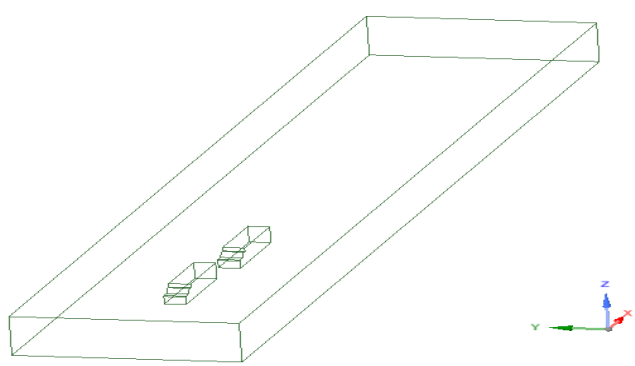

Figure 3. Photo. Illustration of the test body positioning in the computation domain.

The actual computational domain is obtained by subtracting the test bodies from the rectangular enclosure. This is done by performing the Boolean operation in Ansys DM. The hollowed domain is then passed to Ansys Meshing to generate the mesh.

MESHING

Spatial domain discretization is done in Ansys Meshing in a test-improve manner. Ansys Meshing enforces mesh quality with two major criteria: maximum face size and skewness. It performs an adaptive meshing process to refine oversized or ill-shaped elements until the criteria are met. The enforcement criteria are rather basic, and adaptive meshing is often not able to provide satisfactory results, thus requiring manual refinement.

There are three major methods used to improve mesh quality. First, inflation layers are defined on the surfaces of interest, e.g., test body and road surfaces. This approach is widely used in CFD to accommodate large velocity gradients within boundary layers where shear stresses are developed upon contact between fluid and solid surfaces. Finer meshes are required near these boundaries to capture the drastic change in the velocity profile. In Ansys Meshing, inflation layers define surfaces with a series of thin prisms. Figure 4 shows the local meshing implementing inflation layers. These thin prisms are stacked and grow outwards to form a smooth transition to the tetrahedral elements, while making accurate approximation to the near-wall velocity profile.

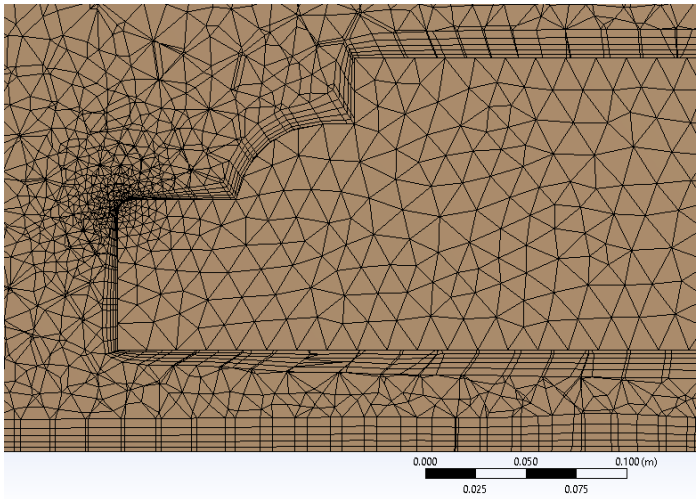

Figure 4. Photo. Illustration of Inflation layers implemented at boundaries.

Second, refinement boxes can be defined in regions where wakes are expected to form. These regions are located behind the truck bodies, where the flow is most turbulent under the separation-convergence motion. Figure 5 presents the mesh after adding a refinement box between the two truck bodies. The mesh maximum face size, defined as the length of the longest edge of an element, is selected to be much smaller within these boxes to achieve higher accuracy.

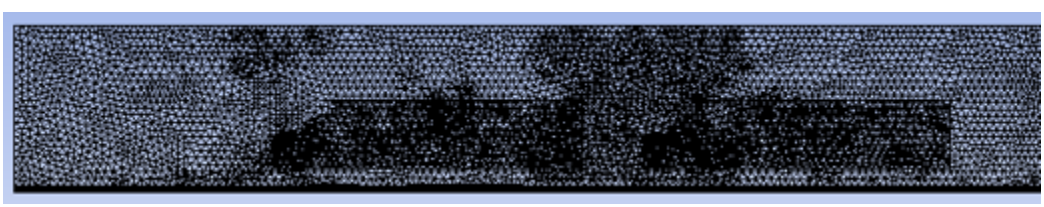

Figure 5. Photo. Illustration of refinement box implemented at wake region.

The third approach is to manually improve mesh quality at low-quality elements by adding partitions or moving nodes. Ansys Meshing provides full control to directly edit elements. This can be labor intensive and is generally used as a last resort when only a small number of elements needs to be treated. Around 1.2 million to 1.5 million elements are generated in each simulation.

FLUENT SETTINGS

The CFD model is Ansys Fluent. The settings used to solve the simulations conform with Ansys Fluent 14 User Guide (2014) and suggestions of CFD researchers (Lanfrit, 2005; Van Leeuwn, 2009). According to the Fluent 14 theoretical guide, the governing equation for incompressible turbulent flow problems is the Reynolds-averaged Navier-Stokes equation (RANS). RANS accurately examines drag force under the influence of a wake with computational efficiency. The turbulence model used is the realizable k-ε model (RKE), which is a two-equation set involving the turbulent kinetic energy (k) and the turbulent dissipation rate (ε). RKE handles turbulent dissipation features in flows with strong curvature and rotation (Lanfrit, 2005), as in the wake region encountered by the trailing truck. The disadvantage of RKE lies in its inability to capture re-lamination (Spalart, 1997). However, this does not significantly impact the result, because re-lamination completes around 150–200 ft behind the truck body (Hinterberger et al. 2004). At this distance, the economic benefit of platooning diminishes, and it is not of interest in this study. For near-wall treatment, nonequilibrium wall functions were used for better handling of separated flows above a moving-wall boundary condition. The solution control settings referred to by Humphreys (2017) and the Ansys Fluent user guide (2014) were also adopted by other researchers such as Van Leeuwen (2009).

To consider the scaled model (1:20) by Reynolds number, the density was set to be 24.5 kg/m^3, which is 20 times the air density at sea level. The reference area was the projected area of the vehicle in the inlet direction. The boundary conditions were defined as follows: velocity inlet was 26.8 m/s (60 mph) on the front of the computational domain; the pressure outlet on the back was 0 Pa; the sides and top areas were symmetry planes; and the road was a moving wall at a velocity of the truck against with the wind (26.8 m/s).

Although the literature provides numerous wind-tunnel test results, these tests were conducted on various types of vehicles (trucks, van, sedans, etc.) with certain aerodynamic features (boat tails, angled taillights, skirts, etc.). The geometric model used in this project is not identical to any of the tests, and very limited tests or simulations are done to examine the effect of lateral offset. However, these test results can be used to validate the CFD simulation, because they are consistent within a small range in terms of the drag coefficient (CD). In addition, simulation results from other CFD support the validation. Figure 6 and Figure 7 show the convergence of the drag coefficient at different separations and zero lateral offset, which agrees with the literature.

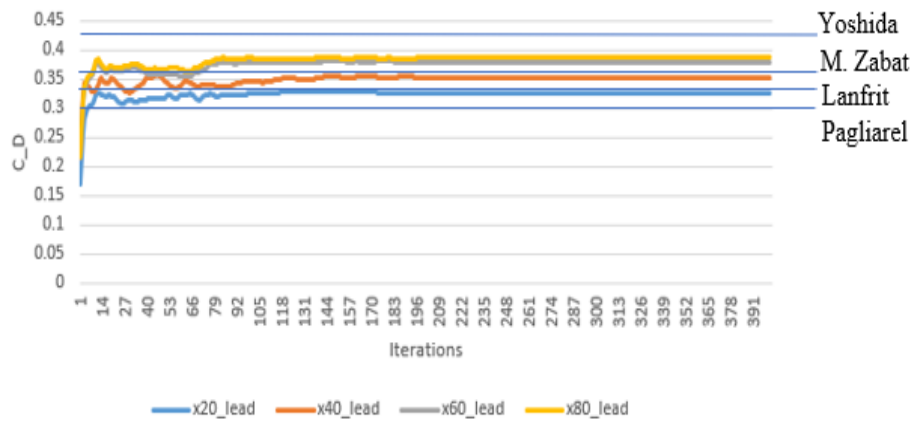

Figure 6. Graph. Drag coefficient of leading truck convergence and validation with literature.

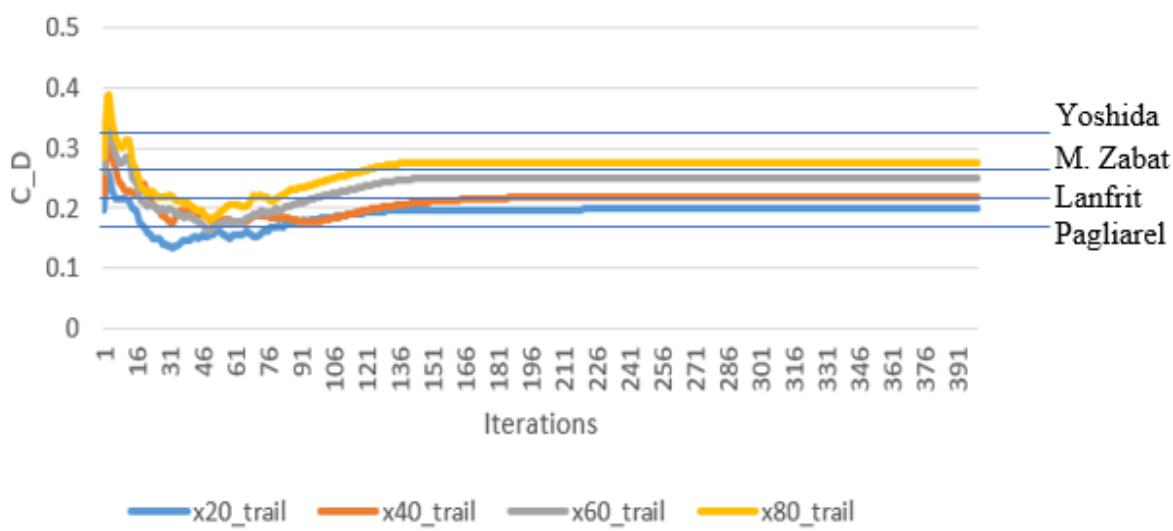

Figure 7. Graph. Drag coefficient of leading truck convergence and validation with literature.

RESULTS

A mesh was designed to evaluate spacing and lateral offset. Figure 8 describes the pressure distribution on the side of the truck and the center plane. The pressure distribution on the truck frontal surfaces with spacing of 11 ft and lateral offset of 1.6 ft is also shown. The pressure distribution on the frontal surface of the trailing vehicle is uneven and is partially outside of the low-pressure region. Consequently, less drag reduction is achieved when a truck is laterally shifted and misaligns with the platoon in front.

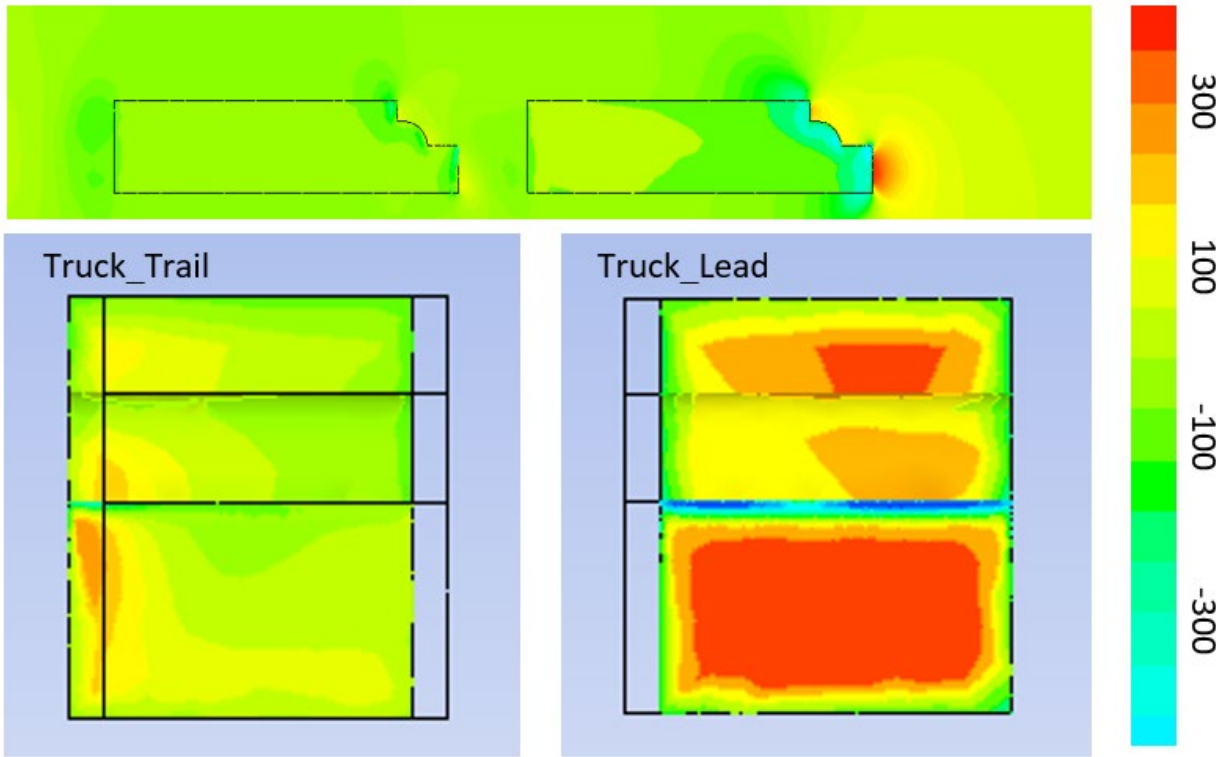

Figure 8. Graph. Pressure contour on the center plain; frontal surface of trailing truck; frontal surface of leading truck.

Figure 9 presents the velocity profile on the center plain between the test bodies, which gives insight to the shape of the wake. The separated flow encountering the rear edges was channeled into a tight but slow vortex, in which much smaller pressure is induced on the frontal surface of the following vehicle. As the distance from the tail increases, flow begins to normalize. An increasing portion is perpendicular to the following vehicle, thus increasing its pressure drag until it reaches that of the leading vehicle.

The front of the vehicle creates a high-pressure region against the flow inlet. The flow is separated by the body from the side and top, leaving a turbulent wake region behind the vehicle. This wake region is of lower pressure and contributes as a pulling force from the rear end. Part of the flow enters a tunnel beneath the vehicle. However, the velocity difference at the two moving boundaries (road and vehicle's bottom) causes this region to be turbulent as well, and it does not contribute to the drag force in the negative direction of motion.

Figure 10 and Figure 11 illustrate the drag ratio over the selected mesh of the design parameters. The drag ration is defined as the ratio of the drag coefficient of the paired truck model (leading and trailing, respectively) to the isolated truck model. This result is fundamental for the prediction model to evaluate gross drag reduction for a platoon, as will be discussed in the following chapter.

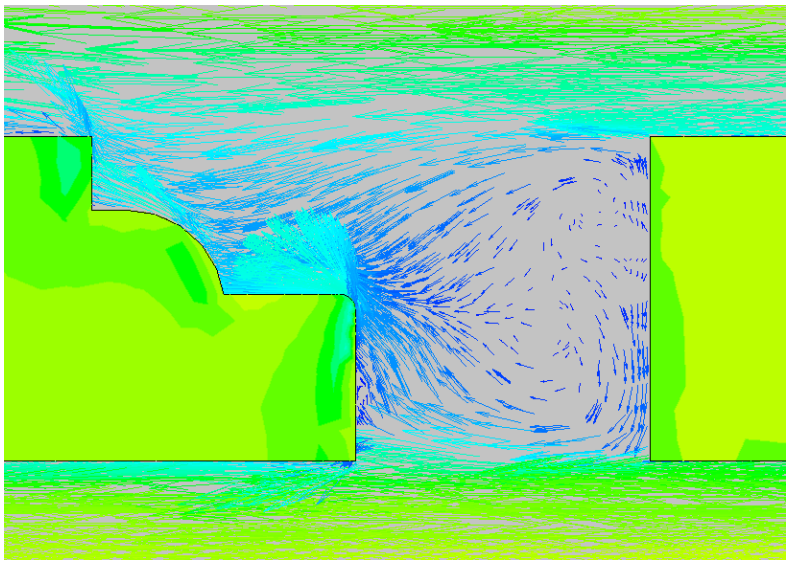

Figure 9. Graph. Velocity vector at wake region between truck bodies.

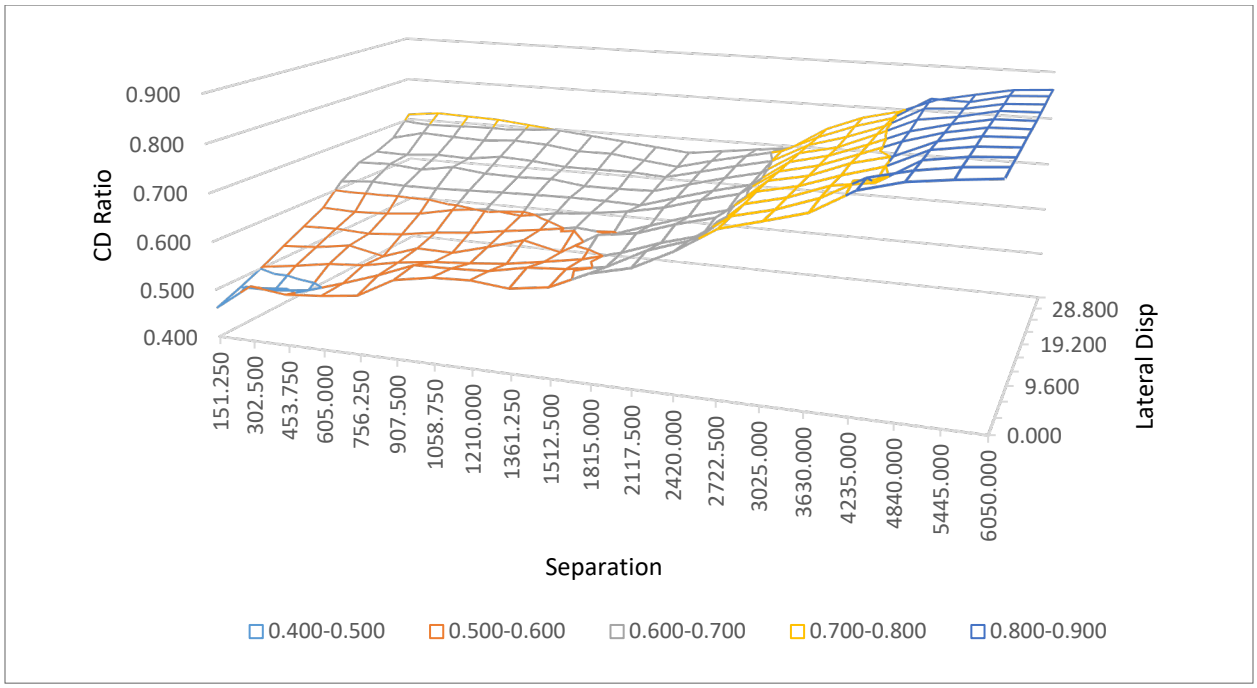

Figure 10. Graph. Surface plot of drag ratio for the trailing vehicle.

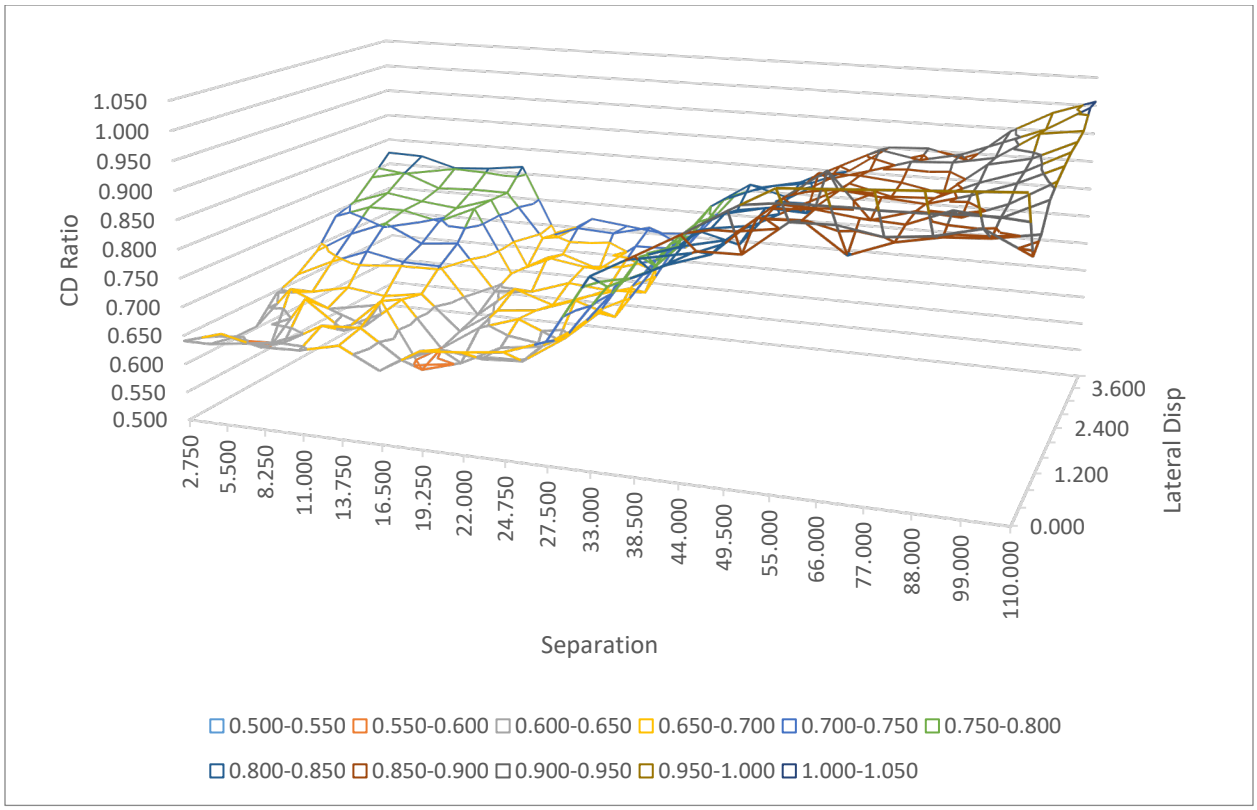

Figure 11. Graph. Surface plot of drag ratio for the leading vehicle.

CHAPTER 3: PREDICTION MODEL IN PLATOONS

OVERVIEW

This section discusses the process of evaluating the user cost due to air drag on several platooned trucks. As previously mentioned, the trailing vehicle compresses the turbulent field behind the leading vehicle and disturbs the rear wake region. The result is a smaller and deviated wake. This is beneficial in two ways. First, it alleviates the negative pressure applied on the rear of the leading vehicle. Second, the trailing vehicle encounters lower pressure compared to the isolated situation. Generally, the vehicles in the middle of a platoon benefit most because the described effects apply to the front and rear end. This is not the case for the leading and last vehicle in the platoon.

FORMULATION

The objective is to design a specific steady-state operation strategy for the driving pattern of the platoon. Intervehicle separations and lateral position of the vehicles within a lane were the inputs. The decision variables are the intervehicle separations S and the lateral positions of the centerline of the vehicles. The spacing s_i is defined as the distance between the rear edge of the ith vehicle and the front edge of the succeeding one. The lateral offset Δx is defined as the absolute displacement of two successive vehicles in the cross-section direction and is calculated as $\Delta x_i = x_i - x_{i-1}$.

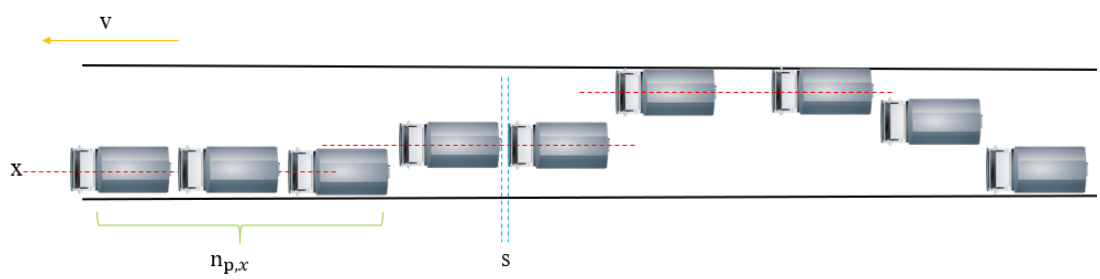

Figure 12. Photo. Illustration of a possible positioning strategy.

The cost is the monetary value per vehicle miles traveled (VMT). The cost is evaluated based on the average energy consumed per mile of cruising, given as Figure 13:

$$cost_{drag}\left(\frac{\$}{VMT}\right) = c_{\mathrm{a}}\frac{1}{2}\rho A C_{D,\infty} v^2 \sum_{n=1}^{N} R_i\,(s, \Delta x)$$

Figure 13. Equation. The operational cost per vehicle-miles-traveled due to air drag.

Where p is the density, v the cruising velocity, A the cross-sectional area of the simulated body, and c_a a conversion factor to dollars per mile, assuming an engine efficiency of 40% and a typical diesel price of 2.8 $/gallon. This quantity is related to the second power of the velocity, as it is derived from energy consumption (third order) but normalized to its unit. The drag ratio R is also influenced by

velocity; however, the velocity was assumed constant at 60 mph in all simulations and was parametrized.

A platoon with more than two vehicles receives asymptotically decreasing drag with the uniform configuration. This was seen in test results reported by Zabat et al. (1995). As shown in Figure 14, closely separated vehicles receive significant drag reduction, and the effect diminishes as separation increases. Air drag decreased asymptotically with the position of a vehicle within a platoon and becomes asymptotic for the fifth vehicle and beyond. The leading and trailing vehicle suffers higher drag than the ones in the middle, as previously mentioned.

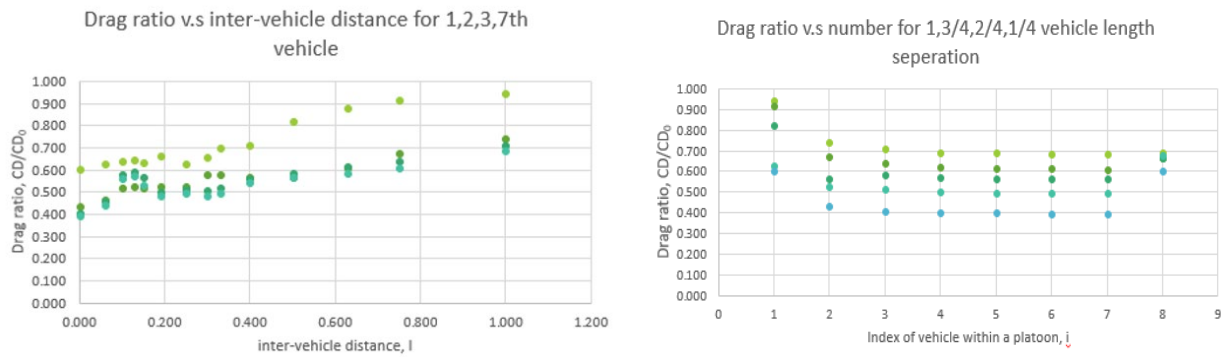

Figure 14. Graph. Drag ratio of platooned vehicles at different separations (Zabat et al., 1995).

It is then necessary to decouple the index *i* and the spatial parameters because *R(s, Δx)* evaluated from CFD analysis on a pair of trucks is not representative as the vehicles inside a platoon are influenced not only by the one in front but all others. The literature has provided meaningful insight into the concepts and effects to consider. However, in this project, the decision variables require continuous domains, thus the positioning mesh needs to be interpolated with curve (surface) fitting. The equation in Figure 15 is proposed as the prediction formula for the drag ratio of the ith truck in the platoon, given the configuration of the preceding trucks:

$$R_i\left(\{s\}_{i-4}^{i-1}, \{\Delta x\}_{i-4}^{i-1}\right) = R_{1,AP} - \sum_{j=1}^{4} a\left(s_{i-j}, \Delta x_{i-j}\right)\Delta R_j$$

Figure 15. Equation. The prediction formula for the drag ratio of the ith truck in platoon.

$$a(s_i, \Delta x_i) = \frac{R_{1,AP} - R_{trail}\,(s_i, \Delta x_i)}{R_{1,AP} - R_{2,AP}}$$

Figure 16. Equation. Correction factor adjusting for the effect of lateral offset.

where $R_{1,AP}$ and $R_{2,AP}$ are the drag reduction of the first and second truck from the test result (Zabat et al., 1995); $R_{trail}(s_i, \Delta x_i)$ is the drag reduction of the trailing truck from the CFD analysis discussed in Chapter 2; ΔR_i is the marginal reduction of the jth preceding vehicle ahead of the evaluated one; and

$a(s_i, \Delta x_i)$ serves as the correcting factor that adjusts the contribution of jth preceding vehicle according to its relative lateral offset. This formulation captures the diminishing influence of misalignment with respect to the position of the truck and the asymptotic behavior of the drag reduction in a large-sized platoon.

SENSITIVITY ANALYSIS

A series of sensitivity analyses is done for platoons with various sizes and uniform configurations. Figure 17 through Figure 21 present the average drag ratio as a function of uniform lateral offset for various separations and platoon sizes. The loss of drag reduction with respect to the lateral offset is close to linear. This is because the geometry of the road, which is generally 12 ft wide, puts a constraint on the 8-ft-wide truck (typical class-8 HDV) so that the maximum lateral offset that may occur is 4 ft (0.5 truck width). This falls in the monotonic smooth region, as observed by Hong et al. (1998). Furthermore, the average drag ratio tends to stabilize for platoons between the sizes of 20 to 30 vehicles. This encourages freight directors to assemble platoons of that size to maximize fuel savings from drag reduction.

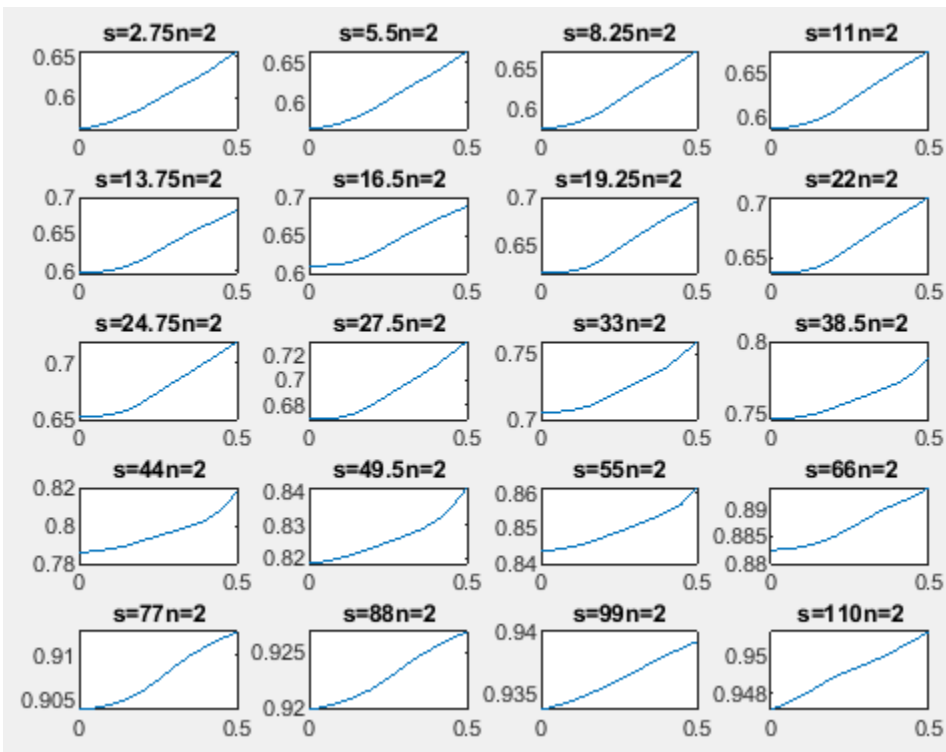

Figure 17. Graph. Sensitivity test on average drag ratio as a function of lateral offset for selected separations and platoons with a size of two vehicles.

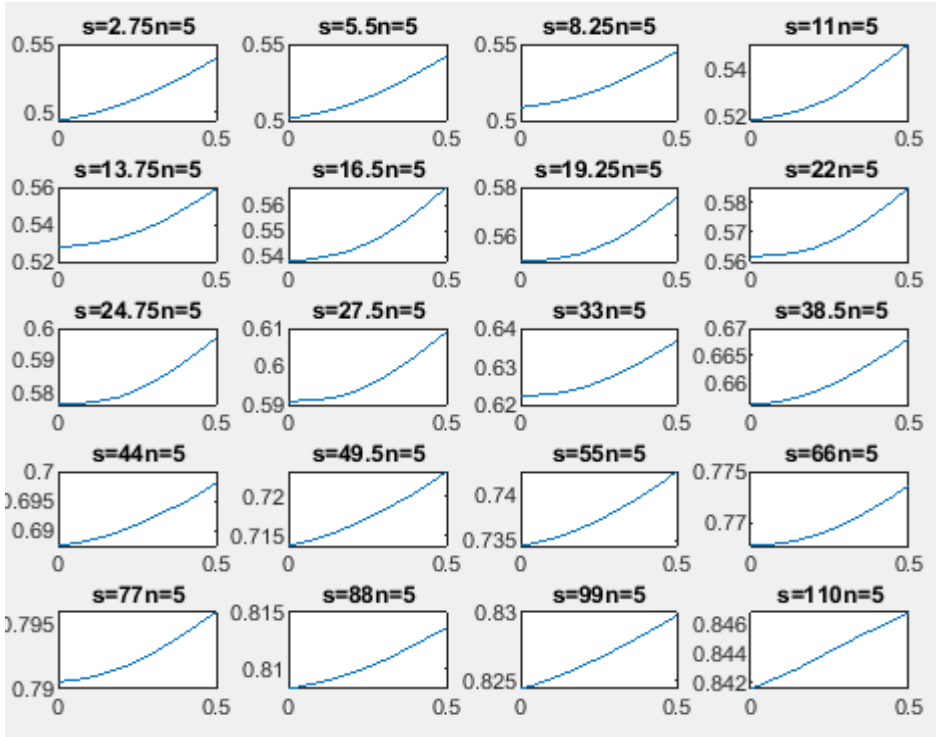

Figure 18. Graph. Sensitivity test on average drag ratio as a function of lateral offset for selected separations and platoons with a size of five vehicles.

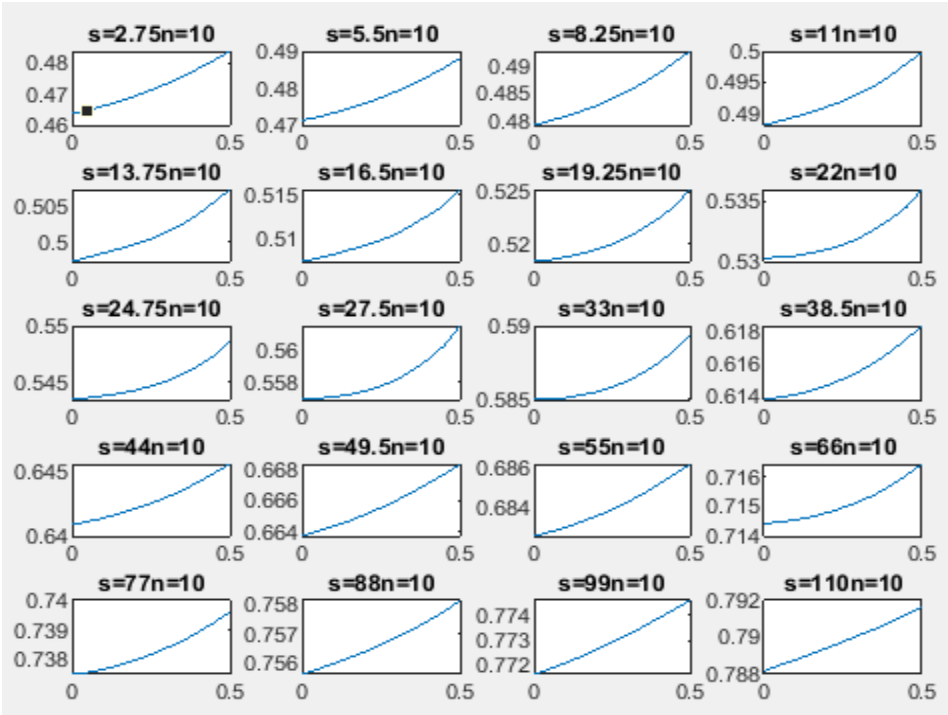

Figure 19. Graph. Sensitivity test on average drag ratio as a function of lateral offset for selected separations and platoons with a size of 10 vehicles.

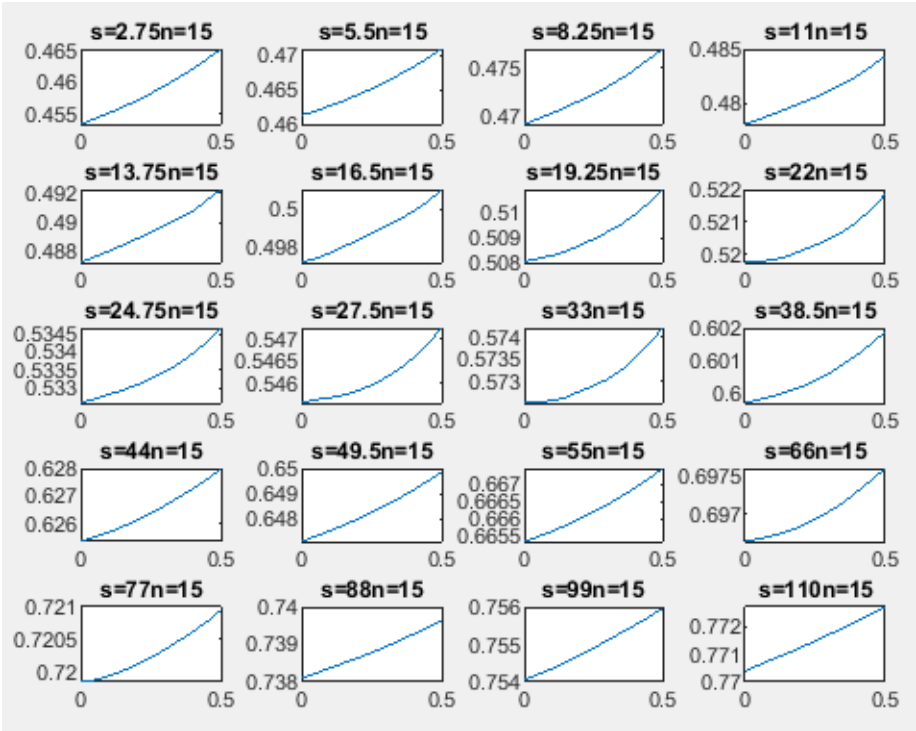

Figure 20. Graph. Sensitivity test on average drag ratio as a function of lateral offset for selected separations and platoons with a size of 15 vehicles.

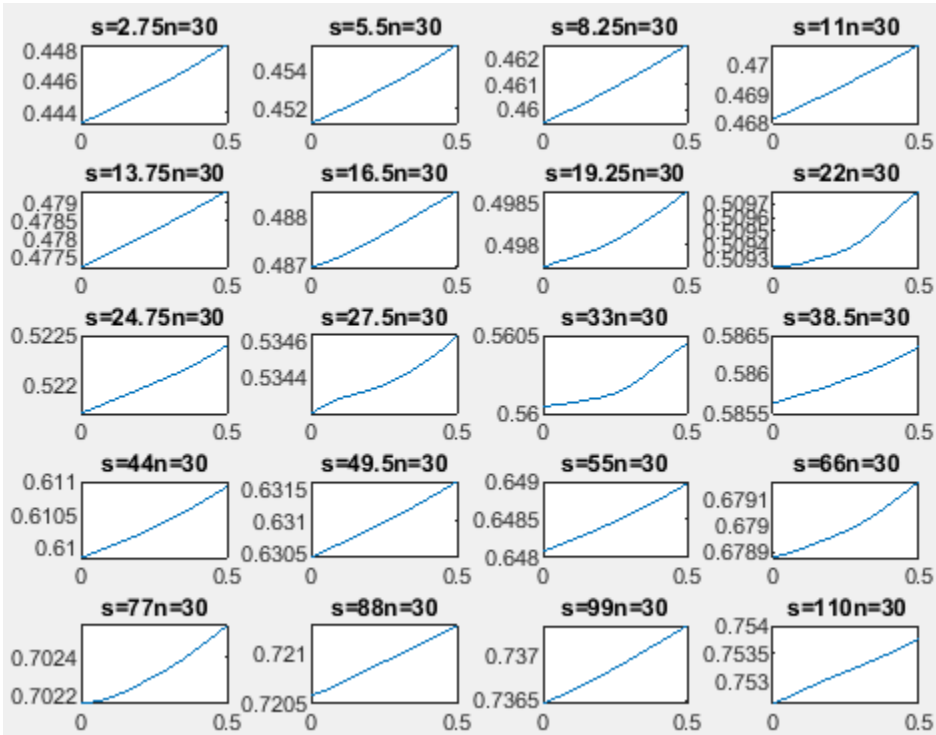

Figure 21. Graph. Sensitivity test on average drag ratio as a function of lateral offset for selected separations and platoons with a size of 30 vehicles.

CHAPTER 4: CONCLUSIONS AND RECOMMENDATIONS

This report aimed to provide a prediction model to evaluate the drag reduction for freight vehicles (class-8 trucks) achieved through platooning. This effect is inspired by CAV technology, which enables small separations between trucks and accurate lateral position control within a lane. Numerous tests have proved the potential savings on fuel consumption from this effect and its significant boost to the freight transportation industry.

To understand and quantify the effect of platoon misalignment (lateral offset) on drag reduction, CFD models simulated pairs of simplified truck bodies using Ansys Fluent. The simulations evaluated the drag force of both leading and trailing trucks in stationary wind and the influence of spatial configuration. This complements CFD studies, where the study of the effect of lateral offset is limited. A prediction formulation was proposed to evaluate the drag ratio of each truck in the platoon given its position and the overall configuration. The results provide insights to the optimal platoon size that maximizes the benefits.

Based on the findings in this report, the following conclusions can be made:

- Freight trucks receive fuel savings between 25–30% because of the aerodynamic effect from platooning. This effect is maximized when trucks are perfectly aligned and closely separated.
- Platooned vehicles receive damped marginal gain when increasing the number trucks. A platoon of 20 to 30 vehicles will receive maximized average drag reduction.

REFERENCES

Ahmed, S., Ramm, G., & Faltin, G. (1984). Some salient features of the time-averaged ground vehicle wake. *SAE Technical Paper*. https://doi.org/10.4271/840300

ANSYS, Inc. (2014). *Ansys fluent 14.0 user's guide* [Report].

Bonnet, C., & Fritz, H. (2014). Fuel consumption reduction in a platoon: Experimental results with two electronically coupled trucks at close spacing. *SAE International*. https://doi.org/10.4271/2000-01-3056

Federal Highway Administration (FHWA). (2004). *Federal size regulations for commercial motor vehicles* [Report].

Hinterberger, C., Garcia-Villalba, M., & Rodi, W. (2004). Large eddy simulation of flow around the Ahmed body. *Aerodynamics of Heavy Vehicles: Trucks, Buses, and Trains*, 19, 77–87.

Hong, P., Marcu, B., Browand, F., & Tucker, A. (1998). Drag forces experienced by two, full-scale vehicles at close spacing. *SAE Technical Paper*. https://doi.org/10.4271/980396

Humphreys, H. (2017). A computational fluid dynamics analysis of a driver-assistive truck platooning system with lateral offset. Unpublished master's thesis, Auburn University.

Lammert, M., Kelly, K., & Walkowicz, K. (2014). Summary of NREL's recent class 8 tractor trailer platooning testing. *21st Century Truck Conference Call*, August 19, 2014.

Lanfrit, M. (2005). A best practice guideline to handle automotive external aerodynamics with FLUENT [Technical notes].

Spalart, P. R. (1997). Comments on the feasibility of LES for wing and on a hybrid RANS/LES approach. In *Proceedings of the First AFOSR International Conference on DNS/LES*.

U.S. Department of Transportation. (2010). *US DOT strategic plan FY2010-FY2015: Transportation for a new generation* [Report].

Van Leeuwen, P. (2009). Computational analysis of base drag reduction using active flow control. Master's thesis, Delft University of Technology.

Yoshida, J., Sugimachi, T., Fukao, Y., & Suzuki, Y. (2010). Autonomous driving of a truck based on path-following control. Presented at the 10th International Symposium on Advanced Vehicle Control, UK, August 22–26, 2010.

Zabat, M., Stabile, N., Farascaroli, S., & Browand, F. (1995). *The aerodynamic performance of platoons: A final report*. California Partners for Advanced Transportation Technology, UC Berkeley.

APPENDIX

Table 1. Tabulated Simulation Result of Drag Ratio of the Trailing Vehicle

CD_ratio_trail												
	delta_x											
		0.000	0.400	0.800	1.200	1.600	2.000	2.400	2.800	3.200	3.600	4.000
s	2.750	0.462	0.481	0.502	0.526	0.549	0.572	0.615	0.642	0.651	0.669	0.712
	5.500	0.515	0.482	0.512	0.531	0.551	0.569	0.620	0.644	0.649	0.686	0.720
	8.250	0.506	0.491	0.524	0.542	0.547	0.572	0.617	0.637	0.655	0.682	0.717
	11.000	0.512	0.514	0.529	0.526	0.553	0.579	0.617	0.649	0.652	0.679	0.714
	13.750	0.521	0.539	0.543	0.551	0.564	0.594	0.619	0.640	0.662	0.684	0.706
	16.500	0.561	0.568	0.552	0.549	0.571	0.603	0.621	0.638	0.658	0.680	0.698
	19.250	0.574	0.569	0.557	0.569	0.582	0.595	0.622	0.640	0.650	0.670	0.691
	22.000	0.577	0.572	0.564	0.591	0.592	0.607	0.623	0.630	0.650	0.670	0.683
	24.750	0.569	0.587	0.576	0.573	0.604	0.615	0.622	0.630	0.650	0.660	0.675
	27.500	0.580	0.592	0.589	0.617	0.597	0.625	0.619	0.632	0.645	0.651	0.667
	33.000	0.615	0.604	0.610	0.628	0.623	0.641	0.642	0.653	0.663	0.671	0.677
	38.500	0.633	0.644	0.637	0.653	0.648	0.664	0.664	0.673	0.682	0.688	0.686
	44.000	0.672	0.670	0.659	0.673	0.668	0.683	0.683	0.692	0.700	0.705	0.696
	49.500	0.721	0.724	0.727	0.732	0.735	0.736	0.738	0.740	0.741	0.742	0.745
	55.000	0.742	0.743	0.746	0.749	0.751	0.754	0.757	0.758	0.764	0.772	0.776
	66.000	0.764	0.771	0.775	0.776	0.782	0.783	0.786	0.791	0.793	0.795	0.795
	77.000	0.810	0.814	0.787	0.799	0.801	0.814	0.818	0.827	0.835	0.842	0.826
	88.000	0.831	0.833	0.834	0.836	0.836	0.837	0.838	0.838	0.840	0.840	0.842
	99.000	0.841	0.845	0.846	0.848	0.851	0.852	0.853	0.855	0.855	0.858	0.857
	110.000	0.849	0.851	0.851	0.852	0.854	0.854	0.855	0.857	0.859	0.862	0.862

Table 2. Tabulated Simulation Result of Drag Ratio of the Leading Vehicle

CD_ratio_lead												
	delta_x											
		0.000	0.400	0.800	1.200	1.600	2.000	2.400	2.800	3.200	3.600	4.000
s	2.750	0.640	0.613	0.603	0.602	0.646	0.662	0.690	0.740	0.753	0.787	0.823
	5.500	0.660	0.622	0.595	0.679	0.655	0.693	0.728	0.764	0.776	0.801	0.820
	8.250	0.645	0.631	0.688	0.651	0.670	0.719	0.755	0.763	0.765	0.775	0.801
	11.000	0.647	0.668	0.638	0.626	0.661	0.705	0.722	0.747	0.757	0.778	0.805
	13.750	0.662	0.671	0.698	0.681	0.671	0.703	0.728	0.778	0.778	0.777	0.814
	16.500	0.627	0.624	0.583	0.599	0.609	0.619	0.644	0.659	0.653	0.692	0.677
	19.250	0.668	0.649	0.603	0.644	0.655	0.675	0.650	0.696	0.684	0.718	0.720
	22.000	0.674	0.641	0.638	0.667	0.662	0.651	0.673	0.685	0.661	0.714	0.711
	24.750	0.682	0.645	0.648	0.638	0.687	0.676	0.666	0.691	0.712	0.731	0.702
	27.500	0.707	0.691	0.691	0.692	0.665	0.696	0.669	0.712	0.714	0.699	0.708
	33.000	0.819	0.783	0.774	0.796	0.761	0.782	0.785	0.787	0.800	0.796	0.790
	38.500	0.858	0.815	0.807	0.820	0.829	0.816	0.825	0.815	0.846	0.825	0.813
	44.000	0.897	0.854	0.830	0.836	0.811	0.826	0.841	0.826	0.827	0.840	0.823
	49.500	0.940	0.855	0.895	0.894	0.896	0.863	0.837	0.893	0.867	0.876	0.852
	55.000	0.979	0.911	0.898	0.899	0.947	0.899	0.895	0.893	0.887	0.911	0.901
	66.000	0.983	0.913	0.848	0.890	0.870	0.892	0.877	0.886	0.908	0.897	0.904
	77.000	0.988	0.900	0.875	0.886	0.891	0.886	0.880	0.872	0.912	0.912	0.886
	88.000	0.992	0.908	0.889	0.914	0.886	0.906	0.912	0.928	0.925	0.939	0.945
	99.000	0.996	0.925	0.893	0.907	0.913	0.931	0.936	0.943	0.972	0.966	0.983
	110.000	1.000	0.889	0.905	0.942	0.955	0.965	0.973	0.976	0.981	1.009	1.007

Table 3. Selected Data from Zabat (1995) on Drag Ratio of Platoons with Extrapolation to the Fifth Truck

CD_ratio_platooned						
	Position Index					
		1	2	3	4	5
s	0.05	0.640	0.462	0.486	0.438	0.448
	0.1	0.660	0.515	0.483	0.434	0.440
	0.15	0.645	0.506	0.478	0.458	0.419
	0.2	0.647	0.512	0.513	0.482	0.472
	0.25	0.662	0.521	0.493	0.461	0.480
	0.3	0.627	0.561	0.513	0.469	0.468
	0.35	0.668	0.574	0.534	0.507	0.503
	0.4	0.674	0.577	0.523	0.500	0.475
	0.45	0.682	0.569	0.537	0.486	0.492
	0.5	0.707	0.580	0.555	0.494	0.510
	0.6	0.819	0.615	0.602	0.555	0.557
	0.7	0.858	0.633	0.634	0.600	0.575
	0.8	0.897	0.672	0.662	0.620	0.599
	0.9	0.940	0.721	0.685	0.658	0.622
	1	0.979	0.742	0.709	0.675	0.639
	1.2	0.983	0.764	0.717	0.679	0.672
	1.4	0.988	0.810	0.754	0.699	0.690
	1.6	0.992	0.831	0.779	0.734	0.725
	1.8	0.996	0.841	0.781	0.716	0.712
	2	1.000	0.849	0.812	0.748	0.735